



Evaluating smartphone-based optical readouts for immunoassays in human and veterinary healthcare: A comparative study

Melania Mesas Gómez^{a,b}, Esther Julián^c, Lara Armengou^d, Maria Isabel Pividori^{a,b,*}

^a Grup de Sensors i Biosensors, Departament de Química, Universitat Autònoma de Barcelona, Bellaterra, Spain

^b Biosensing and Bioanalysis Group, Institute of Biotechnology and Biomedicine, Universitat Autònoma de Barcelona, Bellaterra, Spain

^c Departament de Genètica i de Microbiologia, Facultat de Biociències, Universitat Autònoma de Barcelona, Bellaterra, Spain

^d Fundació Hospital Clínic Veterinari, Universitat Autònoma de Barcelona, Bellaterra, Spain

ARTICLE INFO

Keywords:

Smartphone diagnostics
Bioassay analysis
Colorimetric detection
Mobile health technology
Bacterial detection
Foal immunodeficiencies

ABSTRACT

Recent advances have significantly enhanced the use of smartphone devices for medical diagnostics. This study uses high-resolution cameras in mobile devices to capture and process bioassay images, enabling the quantification of diverse biomarkers across a range of diagnostic tests conducted on 96-well microplates. The study evaluates the effectiveness of this technology through protein quantification techniques and immunoassays that generate colorimetric responses at specific wavelengths. It includes the assessment of bicinchoninic acid and Bradford protein quantification methods, alongside a conventional immunoassay for detecting mare antibodies in colostrum to monitor foal immunodeficiencies. Further application involves the readout of magneto-actuated immunoassays aimed at quantifying bacteria. The results obtained from benchtop spectrophotometry at 595, 562, and 450 nm are compared with those acquired using a smartphone, which identified color intensities in shades of blue, purple, and yellow. This comparison yields promising correlations for the samples tested, suggesting a high degree of accuracy in the smartphone capability to analyze bioassay outcomes. The analysis via smartphone is facilitated by a specific app, which processes the images captured by the phone camera to quantify color intensities corresponding to different biomarker concentrations. Detection limits of 12.3 and 22.8 $\mu\text{g mL}^{-1}$ for the bicinchoninic acid assay and 36.7 and 45.4 $\mu\text{g mL}^{-1}$ for the Bradford are obtained for protein quantification using the spectrophotometer and the smartphone app, respectively. For mare's antibodies in colostrum, the values are 1.14 and 1.72 ng mL^{-1} , while the detection of *E. coli* is performed at 2.0×10^4 and 2.9×10^4 CFU mL^{-1} , respectively. This approach offers further advantages, including wide availability, cost-effectiveness, portability, compared to traditional and expensive benchtop instruments.

1. Introduction

Technological innovation is impacting many societal and scientific aspects with the aim of improving the quality of life. Some trends in mobile digital services have evolved into smaller, more portable smartphones that can connect to several type of networks, with integrated long-lasting batteries. The healthcare sector has also experienced the impact of this technological revolution of mobile health or mHealth, defined by the World Health Organization (WHO) as 'medical and public health practices supported by mobile devices, such as mobile phones, patient monitoring devices, personal digital assistants, and other wireless devices' [1,2]. Ease of monitoring, data collection, and mobile

telemedicine are included among several advantages of mHealth. One particularly interesting aspect is the potential for achieving global health coverage, especially in low- and middle-income countries with hardly accessible areas and limited medical services [3–5]. Some studies suggest that mHealth improves communication and long-term follow-up, allowing a decrease in travel time and offering new forms of cost-effective healthcare [6]. Mobile devices have evolved into versatile and powerful tools for diagnosis and healthcare, enhancing efficiency, accessibility, connectivity, and precision of medical services.

The integration of mobile devices into portable tools with applications that extend beyond biomedical analysis and medical diagnosis has significantly progressed. They are now also used in environmental

* Corresponding author. Grup de Sensors i Biosensors, Unitat de Química Analítica, Universitat Autònoma de Barcelona, Edifici Cn. Campus UAB, 08193, Bellaterra, Barcelona, Spain.

E-mail address: isabel.pividori@uab.cat (M.I. Pividori).

<https://doi.org/10.1016/j.talanta.2024.126106>

Received 25 December 2023; Received in revised form 8 April 2024; Accepted 12 April 2024

Available online 21 April 2024

0039-9140/© 2024 The Authors. Published by Elsevier B.V. This is an open access article under the CC BY license (<http://creativecommons.org/licenses/by/4.0/>).

monitoring and food safety [7–10]. The integration of smartphone-based sensors is a growing trend due to the versatility they offer. This versatility ranges from the use of specialized apps to plug-and-play sensors and more sophisticated commercial kits. For instance, mobile healthcare applications allow users to photograph suspicious lesions and obtain a first evaluation using the phone camera [11]. In the case of environmental monitoring, on-site smartphone-based sensors for the measurement of air pollutants of air quality have been developed. All these approaches use the phone camera as a reader, for example, to determine airborne redox-active compounds [12] or volatile organic compounds [13]. Several options for water quality monitoring are also described, such as the determination of heavy metals in drinking water [14], mapping of nitrite [15] or bisphenol-A [16] contamination, just to mention a few. The integration of high-resolution cameras enables mobile devices to function as optical reading tools in bioanalytical techniques. By taking a photo of the bioassays, the captured images can be further analyzed using specialized software or applications to extract relevant information, such as analyte concentration or the presence of specific biomarkers.

This study demonstrates the use of a mobile phone combined with an application for optical signal processing across different bioassays. Results obtained with the mobile phone were compared to those from a spectrophotometer, which is considered the gold standard. The study was performed on colorimetric assays resulting in differently colored solutions with maximum absorbance peaks at wavelengths such as 450, 562, and 595 nm. These were analyzed using both readout platforms, with 96-well microplates serving as the assay platform for subsequent absorbance reading and imaging to document color intensities. Specifically, the bicinchoninic acid (BCA) (562 nm) and Bradford (595 nm) assays were used as models for protein quantification, widely used in biochemical research, including an enzyme-linked immunosorbent assay (ELISA) (450 nm) designed for quantifying mare antibodies in colostrum samples to control immunodeficiency in foals. Additionally, the mobile phone served as a reader for magneto-actuated immunoassays (450 nm) aimed at detecting and quantifying bacteria, by using modified magnetic particles and simultaneous incubation. Beyond comparing calibration plots from each reading platform, unknown samples were analyzed to determine concentrations and study correlations. The comparison of detection limits (LOD) for each platform is highly promising, highlighting the potential of mobile phones as reading tools. Moreover, the study reveals that, beyond the techniques used, the mobile phone and application can be easily adapted to additional methods, particularly those suited for 96-well microplates that produce colored solutions.

2. Experimental section

2.1. Instrumentation

The optical readout was performed with the spectrophotometer Infinite® M200 PRO using Magellan v4.0 software. The photos of the microplates were taken with the mobile phone iPhone 11 Pro (Apple, Ref. A2215) for further processing using the app Spotxcel® Reader software (Sicasys Software GmbH). The images were taken using a 64 LED light box with USB power supply to control the lighting conditions with a distance from the mobile camera to the plate of 23 cm, applying the white lights (T~6500K) with a 14 W power. The selection of 6500K white light for our mobile imaging setup, simulating natural daylight with a broad spectrum (400–700 nm), ensures accurate color representation and differentiation in bioassay readouts, essential for precise scientific analysis. Further instrumentation details are provided in S1 (Supp. Data).

2.2. Chemicals and biochemicals

The protein quantification tests were performed with the kit ThermoScientific™ Pierce™ BCA Protein Assay (ThermoFisher Scientific, Ref. 23227) and the Pierce™ Coomassie (Bradford) Protein Assay Kit (ThermoFisher Scientific, Ref. 23200), using BSA standards (ThermoFisher Scientific, Ref. 23209). ELISAs were conducted using the following antibodies: anti-horse IgG (Fc specific) produced in rabbit (Ref. SAB3700150, Sigma-Aldrich) as a capture antibody and anti-Horse IgG H&L labelled with horseradish peroxidase (HRP) produced in rabbit (Ref. ab102405, Abcam) for labelling. The sample used was a colostrum pool quantified by radial immunodiffusion with a total value of 16820 mg dL⁻¹ horse antibodies. M450 tosyl activated magnetic particles (Dynabeads™ M – 450 Tosylactivated, Catalogue no. 14013, Invitrogen) were used for immobilizing polyclonal anti-*E. coli* antibodies (Ref. ab137967, Abcam) from rabbit. The rabbit polyclonal anti-*E. coli* labelled with HRP (Ref. ab20425, Abcam) was used as a secondary antibody. The HRP enzyme (Ref. 77332, Roche) was used to prepare the solutions for reproducibility assay. For all immunoassays, TMB Substrate Kit (Ref. 34021, Thermo Scientific Pierce) were used for the enzymatic reaction and color development, and a 2.0 M solution of sulfuric acid was used to stop the TMB reaction. The bacterial culture reagents were purchased from Sigma, including Luria Bertani (LB) medium (Ref. L3522) and LB-agar plates (Ref. L3147-250G) for *E. coli* growing. Different sets of buffers were used for each experiment, and their compositions are described in S1 (Supp. Data). All buffers were prepared from chemicals of analytical grade purchased from Merck and Sigma and using milliQ water. Colostrum samples used in this study were exclusively leftovers from colostrum obtained from mares by manual milking, during the standard procedure of colostrum quality assessment immediately after parturition, a non-invasive and routine procedure in equine care conducted at the Fundació Hospital Clínic Veterinari, Universitat Autònoma de Barcelona (Spain).

2.3. Bicinchoninic acid and Bradford assays for protein quantification

A calibration curve was prepared for the quantification of protein samples based on the Bicinchoninic Acid (BCA) and the Bradford method, starting from a known concentration standard of BSA as a protein model, ranging from 0 to 2000 µg mL⁻¹. In addition, 48 samples of unknown BSA concentration were quantified and interpolated onto the curves obtained by each method. The detailed protocol and fundamentals for BCA are described in Fig. S2 (Supp. data). The optical readout was performed at 562 nm with the spectrophotometer. Images were also taken with the mobile phone to quantify the purple color intensity using the app. The detailed protocol and fundamentals for the Bradford assay are described in Fig. S3 (Supp. data). In this instance, the optical readout was performed at 595 nm with the spectrophotometer and the images were quantified by the blue color intensity with the mobile app.

2.4. Enzyme-linked immunosorbent assay for quantification of IgG in colostrum from mares

The detection of IgG in colostrum samples was used as model for enzyme-linked immunosorbent assay (ELISA). More details about the ELISA protocol are described in S4 (Supp. Data). A calibration curve from a colostrum pool with a known concentration of antibodies was performed in a range of 0–8.41 µg mL⁻¹. In addition, 40 colostrum unknown samples were quantified and interpolated in the curve. The signals obtained were quantified by measuring the absorbance at 450 nm with the spectrophotometer and photos of the microplate were taken with the mobile phone to quantify the yellow color intensity with the mobile app.

2.5. Magneto-actuated immunoassay for the detection of *E. coli*

Escherichia coli (CECT 405, ATCC 10536) was used as a model of gram-negative bacteria. The bacteria were grown in a liquid culture at 37 °C for 24 h until they reached an OD of 1.000 AU at 550 nm. The bacteria were inoculated in PBS for the preparation of the samples and the concentration was calculated by colony counts verification in solid culture. The quantification of bacteria in liquid samples using a magneto-actuated immunoassay was used as a model in order to evaluate the versatility of the mobile phone as a portable optical reader. A simultaneous magneto-ELISA for the detection of *E. coli* was performed and the details of the procedure are described in S5 (Supp. Data). Briefly, one-step incubation of all the reagents, including antiEcoli-MPs and the enzymatic conjugate antiEcoli-HRP antibodies and 100 µL of *E. coli* samples was performed in agitation at RT for 1 h, followed by washing and the enzymatic reaction. The readout is performed either by reading the absorbance at 450 nm in the spectrophotometer and by taking an image of the microplate to quantify the yellow color intensity with the mobile app. A calibration curve was performed from 0 to 3×10^8 CFU mL⁻¹ and 14 unknown samples were also analyzed.

2.6. Reproducibility study of the optical readout for the individual wells in a 96-well microplate

In order to study the reproducibility of the readout, the same solution was dispensed at the same volume in each well of a 96-well microplate, in order to evaluate possible effects when taking and processing the image with the mobile application, including distance from the microplate and the incident light, position of the well within the microplate, light intensity, reproducibility of the microplate, among other factors. For this purpose, two readout platforms were studied by preparing two bulk solutions (purple color/ λ 562 nm and yellow color/ λ 450 nm). To achieve that, a known BSA sample of 1 mg mL⁻¹ was incubated with the BCA reagent at 37 °C for 30 min. Finally, 200 µL of the same solution was dispensed in each of the 96 wells of the microplate for further readout at 562 nm and purple color intensity with the mobile app.

On the other hand, HRP at 0.02 U mL⁻¹ was incubated with TMB/H₂O₂ (1:1) substrates for 10 min and the reaction was stopped with acid. Finally, 200 µL of the same solution was dispensed in each of the 96 wells of the microplate for further readout at 450 nm and yellow color intensity with the mobile app.

2.7. Image treatment and statistical analysis

In all instances, to ensure uniform illumination for mobile imaging across all experiments, photographs were taken under consistent lighting conditions. A light box with white walls was used to facilitate equal light diffusion, thereby maintaining steady light intensity and color temperature for every photograph. This setup aimed to guarantee a uniform background and consistent white balance throughout all images. Furthermore, to achieve maximum uniformity, all photographs were captured using the same mobile device, an iPhone 11 Pro by Apple, ensuring uniform photographic conditions and the use of the same camera sensor. The distance between the microplate and the camera of the mobile phone was consistently maintained at 23 cm, according to the geometry of the light box. Similarly, the placement of the microplate inside the light box was standardized, along with the utilization of identical lighting conditions for each assay, including white light at 6500 K and a power of 14 W, to ensure assay reproducibility. The photographs were captured at a resolution of 12 megapixels using the phone default zoom (x1). The camera flash was turned off to avoid glare, and the focus was set to automatic, further contributing to the consistency and reliability of the imaging process. The iPhone 11 Pro used in this study features a 12 MPx triple-camera system. This device supports wide color gamut technology and employs a high-quality CMOS sensor, offering exceptional sensitivity to capture a broad spectrum of colors.

Coupled with sophisticated color calibration and image processing algorithms, it ensures precise color differentiation and accuracy, even in subtle variations. The images were stored in the internal memory and later processed with the Spotxel® Reader mobile application, as described in S6 (Supp. Data). Briefly, the image to be processed was selected and uploaded in the mobile application, and the 96-well virtual microplate was aligned with the image. The grid's distortion factor was applied, and the measuring color was selected depending on the assay (yellow, blue, or purple). Finally, the intensity of the color in each well was quantified by the mobile app to obtain the relative signal value in color. The color intensity values were obtained in arbitrary units, for to be further analyzed with Prism v 10.0.1 (GraphPad, San Diego, USA). The readout color mode selected in the app was yellow for the immunoassays, purple for the BCA test, or blue for Bradford tests. The absorbance was also measured in the spectrophotometer corresponding to the wavelengths of maximum absorption for each assay, 450, 562, and 595 nm, respectively. The statistical analyses were performed using Prism v 10.0.1 (GraphPad, San Diego, USA). To compare the data obtained by both readout platforms, the values obtained were previously normalized from 0 to 100, for the minimum to the maximum value. The calibration curves were adjusted to a non-linear regression fitting, using the four-parameter logistic curve, abbreviated 4 PL. Each concentration was analyzed per triplicate. The limit of detection (LOD) was calculated as considering the number of negative controls for each curve, using the one-tailed test with a significance level of $p < 0.05$ (Student's t , $p < 0.05$). The limit of quantification (LOQ) was determined by calculating the blank signal as $10\sigma_{blank} + \bar{x}_{blank}$ and interpolating the value into the curve. For the analysis of the unknown samples, the concentrations obtained from each readout method were plotted on a linear regression graph to calculate the correlation coefficient (R^2). The x-axis represented the data from the gold standard spectrophotometric method, while the y-axis represented the data from the mobile phone and app platform.

2.8. Biosafety considerations

The experiments were performed according to Biosafety Class 2 required for the handling of *E. coli*. All biological waste generated from the experiments were disposed in accordance with the local regulations for handling biohazards.

3. Results and discussion

3.1. Study of the mobile phone as readout platform in bicinchoninic acid and Bradford assays for protein quantification

Bicinchoninic acid (BCA) assay (or Smith assay) for total protein quantification relies on the formation of a Cu²⁺-protein complex in a basic medium, followed by the reduction of the Cu²⁺ to Cu⁺ [17]. The Cu²⁺ that is reduced is proportional to the protein in the solution. Basically, two molecules of BCA chelate to each Cu⁺ ion causing a change of color from green to purple with a strong absorbance at 562 nm, as shown in Fig. S2 (Supp. data). The bicinchoninic Cu⁺ complex is influenced by the number of peptide bonds, and the presence of amino acids as cysteine, cystine, tyrosine, and tryptophan side chains [18]. The assay was developed in 96-well microplates and the readout was achieved at 562 nm with the spectrophotometer and with the mobile phone in the purple color intensity mode of the mobile app, and the results are shown in Fig. 1, panel A.

The Bradford assay is a rapid and sensitive method for measuring the concentrations of proteins. It is based on the shift in absorbance maximum of the anionic form of Coomassie Brilliant Blue G-250 dye from 465 to 595 nm following binding to arginine and lysine residues of proteins in solution [19], as shown in Fig. S3 (Supp. data). The assay was developed in 96-well microplates and the readout was achieved at 595 nm with the spectrophotometer and with the mobile phone in the blue

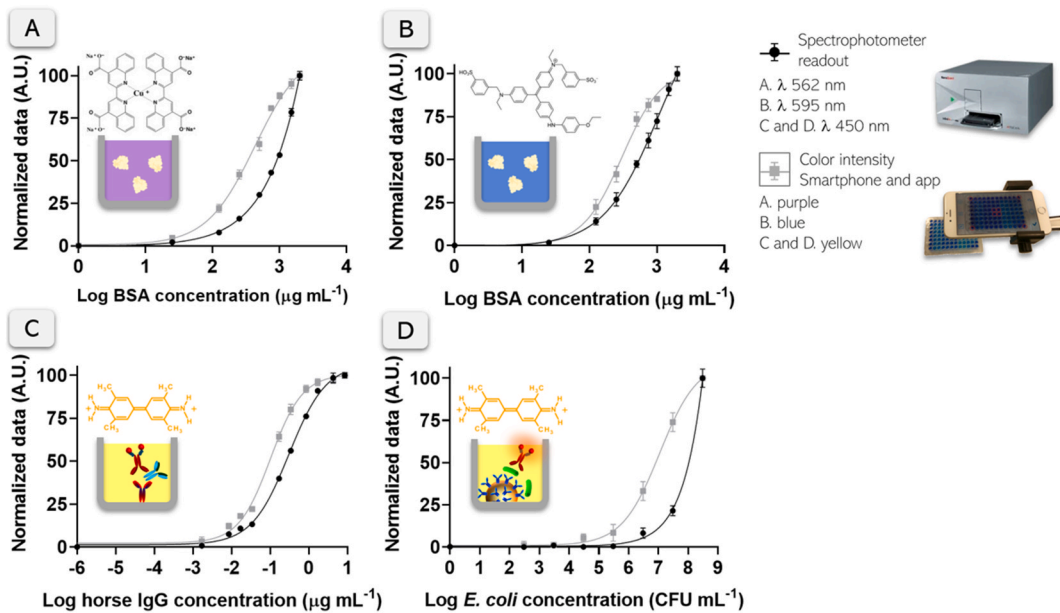


Fig. 1. Calibration plots and fundamentals for each determination performed in 96-well microplates with the mobile phone and app platform (gray squares) compared with the gold standard spectrophotometer (black circles). Panel A. Bicinchoninic acid for protein quantification (purple color/ $\lambda = 562$ nm, respectively). Panel B. Bradford assay for protein quantification (blue color/ $\lambda = 595$ nm, respectively). Panel C. Enzyme-linked immunosorbent assay for quantification of IgG in colostrum from mares. Panel D. Magneto-actuated immunoassay for the detection of *E. coli*. The readout in Panels C and D was performed in yellow color and $\lambda = 450$ nm. In all cases, $n = 3$.

color intensity mode of the mobile app, and the results are shown in Fig. 1, panel B.

In both instances, it is observed that the calibration plot obtained with the mobile phone and app platform saturate at lower concentration, which indicates a lower dynamic range. However, the signals obtained at lower concentration ranges were comparatively higher with the mobile phone than the spectrophotometer, reaching an order of magnitude less for the LOQ, especially in the case of BCA. The LOD calculated for each readout system were found to be of the same order of magnitude and very similar among them for both wavelengths and colors, obtaining values as 12.3 and $22.8 \mu\text{g mL}^{-1}$ for the BCA assay ($\lambda = 562$ nm, purple color) and, 36.7 and $45.4 \mu\text{g mL}^{-1}$ for the Bradford assay ($\lambda = 595$ nm, blue color), for the spectrophotometer and the mobile phone, respectively. All calculated values related with the analytical performance of both methods are comparatively summarized in Table 1.

The analysis of the results for the Bradford assay exhibited a good correlation of 0.8845 , and up to 0.9527 for the BCA assay, as shown in Fig. 2, panel B and A, respectively.

3.2. Study of the mobile phone as readout platform in the enzyme-linked immunosorbent assay for quantification of IgG in colostrum from mares

Horseradish peroxidase (HRP) is a widely employed enzyme label in immunoassays, since it offers a range of significant advantages. These include a high turnover rate and the ability to amplify signals, increasing the sensitivity. Moreover, HRP has a long shelf life, ensuring the stability of labelled reagents. Its versatility is another key asset, as HRP readily conjugates with many proteins, enabling diverse immunoassay formats. The enzyme compatibility with standard laboratory equipment enhances accessibility and simplifies implementation even in low-resource setting. Additionally, HRP displays low levels of nonspecific adsorption. In this instance, an immunoassay model with a TMB substrate solution was used to quantify mare antibodies in colostrum samples for the monitoring of foals, based on HRP-labelled antibodies and TMB- H_2O_2 substrate, producing a yellow solution with a maximum absorbance peak at 450 nm. An effective transfer of antibodies from the mare through colostrum plays a pivotal role in providing the foal with

Table 1

Summary of the calculated values from the data analysis of the calibration curves obtained by the spectrophotometer and the mobile phone for each technique. The calculated parameters were the R square for the adjustment of the four-parameter logistic curve fitting, limit of detection (LOD), limit of quantification (LOQ) and the correlation of the unknown samples analyzed by each reading platform.

	Absorbance/ Spectrophotometer	Color intensity/ Mobile phone
BCA Assay	562 nm	Purple color
R square	0.9988	0.9944
LOD ($\mu\text{g}\cdot\text{mL}^{-1}$)	12.3 (n = 8)	22.8 (n = 8)
LOQ ($\mu\text{g}\cdot\text{mL}^{-1}$)	50.3	116
Correlation in calculated unknown samples (n = 47)	0.9527	
Bradford assay	595 nm	Blue
R square	0.9940	0.9905
LOD ($\mu\text{g}\cdot\text{mL}^{-1}$)	36.7 (n = 6)	45.4 (n = 6)
LOQ ($\mu\text{g}\cdot\text{mL}^{-1}$)	138	136
Correlation in calculated unknown samples (n = 40)	0.8845	
Immunoassays	450 nm	Yellow
	ELISA for quantification of IgG in colostrum from mares	
R square	0.9978	0.9958
LOD ($\text{ng}\cdot\text{mL}^{-1}$)	1.14 (n = 9)	1.72 (n = 9)
LOQ ($\text{ng}\cdot\text{mL}^{-1}$)	26.7	27.3
Correlation in calculated unknown samples (n = 40)	0.8954	
	Magneto-ELISA for the detection of <i>E. coli</i>	
R square	0.9942	0.9937
LOD ($\text{CFU}\cdot\text{mL}^{-1}$)	$2.0\cdot 10^4$ (n = 6)	$2.9\cdot 10^4$ (n = 6)
LOQ ($\text{CFU}\cdot\text{mL}^{-1}$)	$1.2\cdot 10^6$	$7.7\cdot 10^5$
Correlation in calculated unknown samples (n = 14)	0.9144	

sufficient passive immunity and protection against viruses and bacteria, reducing the risk of developing serious medical conditions [20,21]. Hence, monitoring, and quantifying antibodies in colostrum are crucial for ensuring the health of foals. In Fig. 1, panel C it was remarkable the similar fitting of both calibration curves for the conventional

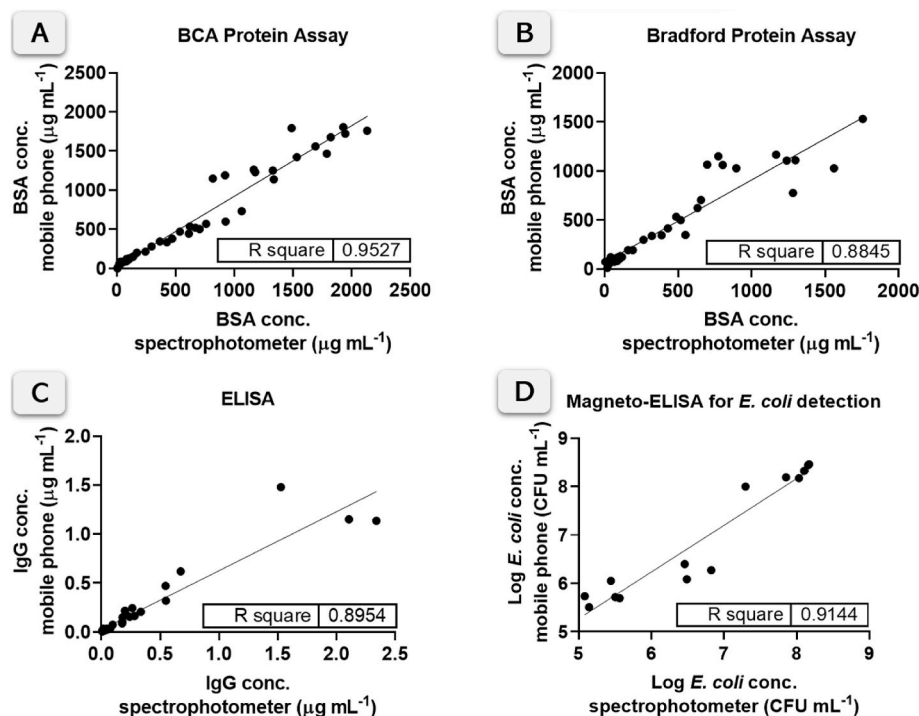


Fig. 2. Correlation plots for each determination performed in 96-well microplates with the mobile phone and app platform (y-axis) compared with the gold standard spectrophotometer (x-axis). Panel A. Bicinchoninic acid for protein quantification (purple color/ $\lambda = 562$ nm, respectively). Panel B. Bradford assay for protein quantification (blue color/ $\lambda = 595$ nm, respectively). Panel C. Enzyme-linked immunosorbent assay for quantification of IgG in colostrum from mares. Panel D. Magneto-actuated immunoassay for the detection of *E. coli*. The readout in Panels C and D was performed in yellow color and $\lambda = 450$ nm.

immunoassay. Similar to the curves obtained by BCA and Bradford methods, the curve obtained using the mobile phone saturates before that of the spectrophotometer, slightly reducing the dynamic range. Both LOD and LOQ were very similar for the two readout platforms, obtaining values as 1.14 and 1.72 for the LOD and 26.7 and 27.3 ng mL^{-1} for the LOQ, obtained by the spectrophotometer and the mobile phone, respectively. The analysis of the unknown samples for the ELISA also exhibited a good correlation between both reading platforms of 0.8954 (Table 1 and Fig. 2, panel C).

3.3. Study of the mobile phone as readout platform in magneto-actuated immunoassay for the detection of *E. coli*

In this work, the ability of the mobile phone as readout platform was also evaluated based on a magneto-actuated immunoassay [22,23] for the detection and quantification of *E. coli*, producing a yellow solution with maximum absorbance at 450 nm, as in the case of a conventional immunoassay. The results showed a similar pattern in the calibration plots after the fitting (Fig. 1, panel D), although the dynamic range with the mobile phone was found to be lower as the saturation of the curve was reached at a lower concentration in comparison with the spectrophotometer, as described above. But as in the previous examples, at lower concentration ranges, the signals were significantly higher for the curves obtained with the mobile phone compared to the spectrophotometer. Accordingly, the LOQ for the magneto-actuated immunoassay was found to be lower with the mobile phone readout (Table 1). However, the LOD was found to be comparable between those calculated with the mobile phone and the spectrophotometer. In addition, the analysis of the samples of unknown concentration showed a good correlation between both readout platforms of 0.9144 (Fig. 2, panel D).

3.4. Reproducibility study of the optical readout for the individual wells in a 96-well microplate

In this work, the reproducibility of the optical readout for the individual wells in a 96-well microplate was studied at 450 nm (yellow) and 562 nm (purple) by preparing a bulk large volume solution and by dispensing the same solution on each well. In all instances, the signals were normalized in order to maximize the small differences of the plates. As the solution is the same in all cases, the differences of signals in the wells can be attributed to other systematic errors such as light conditions, microplate geometry, image acquiring or data processing among others. As shown in Fig. 3 panel B and E, a similar circle-shaped pattern in the signal can be observed in the center of the microplates when analyzed with the mobile phone. While this pattern was much more noticeable in the case of the purple color intensity (panel E), it was also slightly observed in the case of the yellow color intensity (panel B). This pattern of signals was not observed in the absorbance measurements neither for the assay in yellow color and $\lambda = 450$ nm, nor with the purple color and $\lambda = 562$ nm, respectively, represented in Fig. 3, panel A and D, respectively. The signal difference in these last cases seems to be random, without a specific pattern in the variation of the absorbance values. As described, the images of the microplates were taken in controlled lighting conditions, under a LED light circular-shaped. However, it must be noted that the variability between signals, both in absorbance and color intensity, was found to be very small, although it was magnified by normalization in Fig. 3 to identify possible patterns. Accordingly, 0 and 100 % were attributed to the minimum and maximum value obtained, respectively. In addition, as has been verified in the previous sections, the use of the mobile phone as an optical readout platform resulted very promising, obtaining calibration curves with similar fittings to those obtained with the spectrophotometer, just like the calculated LOD and LOQ.

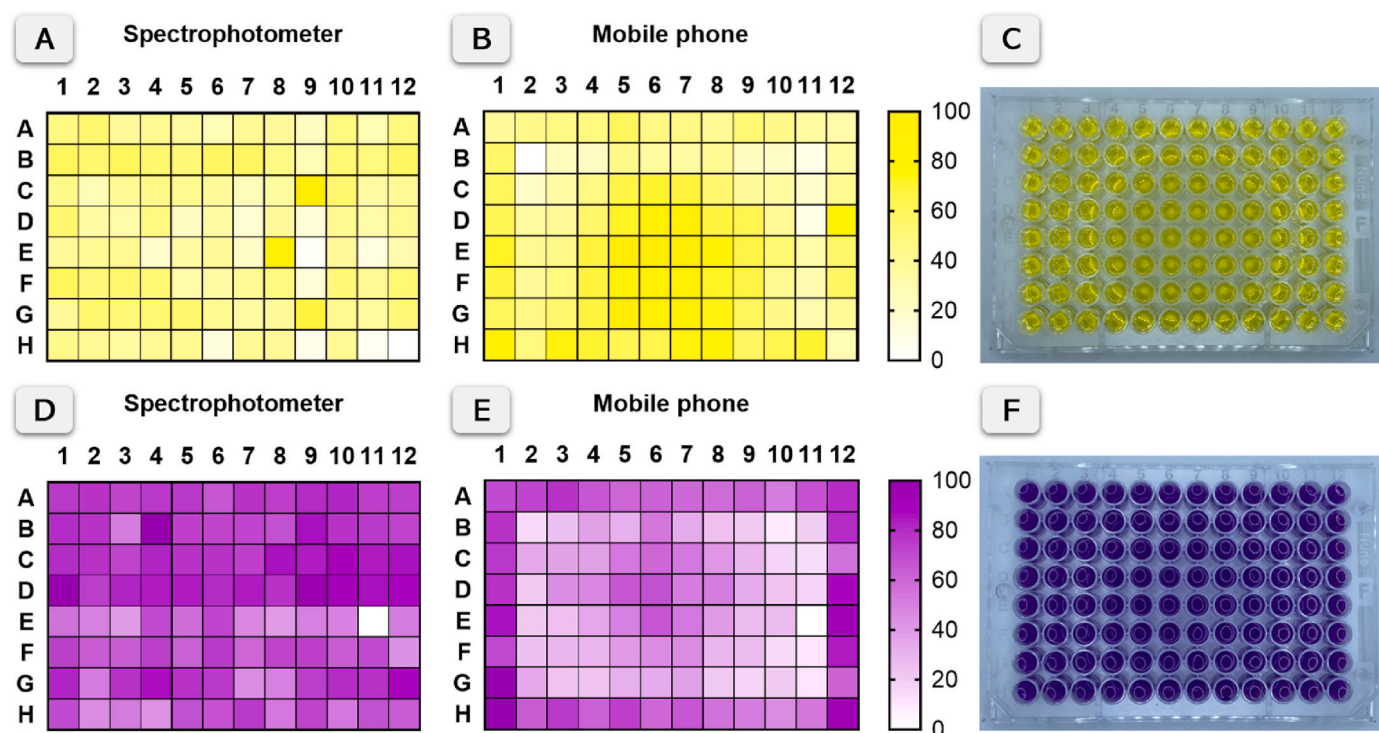


Fig. 3. Schematic heat-map of 96-well microplates representation of the results obtained for the reproducibility test after data normalization of the absorbance with the spectrophotometer and the color intensity by the mobile phone. The panels show the results obtained for panel A) absorbance measurement at 450 nm, B) intensity of yellow color signal and C) image of the 96-well plate with the yellow solution. On the other hand, the results obtained for panel D) absorbance measurement at 562 nm, E) intensity of purple color signal and F) image of the 96-well plate with the purple solution.

3.5. Conclusions

Portability, connectivity, ease of use, and affordability are just some of the advantages that make the use of mobile devices increasingly integrated as portable analysis tools, whether in several applications in medicine, food safety or environmental monitoring [24]. This study explores the smartphone capability as an optical readout platform for widely used biochemistry techniques, such as BCA and Bradford assays, ELISA for quantifying mare antibodies, and magneto-actuated immunoassays for bacterial detection. Utilizing a mobile app for direct processing or uploading microplate photos, the results show promising comparability with spectrophotometer results, including similar limits of detection and quantification. Notably, proper lighting control emerged as essential for accurate image capture. The versatility of the app, offering various color measurement options, demonstrates potential for broader application in colorimetric tests, presenting a cost-effective alternative to traditional benchtop instruments. The novelty of integrating smartphone technology in immunoassay readouts is highlighted in this manuscript, representing a significant advance in the diagnostic field in low-resource settings. This study is characterized by the application of mobile devices to quantify different targets in a diverse range of bioassays, highlighting the versatile utility of smartphones beyond their conventional uses. The efficacy of this approach across multiple assay types is comprehensively evaluated, demonstrating its broad applicability in the domains of human and veterinary health. A key aspect of the research is the implementation of advanced image processing within mobile app, designed to interpret bioassay results with outstanding performance. Such innovation marks a substantial progression in the capabilities of mobile health diagnostics. Moreover, a rigorous comparative analysis with traditional benchtop spectrophotometers has validated the reliability of smartphone-based readouts, showing comparable limits of detection and accuracy. The emphasis on applications for both human and veterinary health expands the potential of this approach to change diagnostic practices, especially

in scarce-resource settings. This contribution establishes a basis for future advance in accessible, efficient, and accurate mobile diagnostics, highlighting the significant role of smartphones in the progression of healthcare technologies.

CRediT authorship contribution statement

Melania Mesas Gómez: Writing – original draft, Validation, Investigation, Formal analysis, Data curation. **Esther Julián:** Supervision, Investigation. **Lara Armengou:** Supervision, Investigation. **Maria Isabel Pividori:** Writing – review & editing, Supervision, Methodology, Funding acquisition, Conceptualization.

Declaration of competing interest

The authors declare that they have no known competing financial interests or personal relationships that could have appeared to influence the work reported in this paper.

Data availability

Data will be made available on request.

Acknowledgments

This research was funded by the Ministry of Science, Innovation and Universities, Spain (Projects PID2019-106625RB-I00/AEI/10.13039/501100011033 and PID2022-136453OB-I00) and from Generalitat de Catalunya (2017-SGR-220 and 2021SGR-00124, 2021SGR-00092). Also, Ministry of Universities (Grant FPI/BES- 2017-080748) are gratefully acknowledged. The JM Horse Farm for providing the colostrum samples is also gratefully acknowledged.

Appendix A. Supplementary data

Supplementary data to this article can be found online at <https://doi.org/10.1016/j.talanta.2024.126106>.

References

- [1] WHO Global Observatory for eHealth, mHealth: New Horizons for Health through Mobile Technologies: Second Global Survey on eHealth, World Health Organization, 2011. <https://iris.who.int/handle/10665/44607>.
- [2] S.P. Rowland, J.E. Fitzgerald, T. Holme, J. Powell, A. McGregor, What is the clinical value of mHealth for patients? *Npj Digit. Med.* 3 (2020) 4, <https://doi.org/10.1038/s41746-019-0206-x>.
- [3] H. Ayatollahi, Point-of-care diagnostics with smartphone, in: *Smartphone-Based Detect. Devices*, Elsevier, 2021, pp. 363–374, <https://doi.org/10.1016/b978-0-12-823696-3.00017-9>.
- [4] K. Källander, J.K. Tibenderana, O.J. Akpogheneta, D.L. Strachan, Z. Hill, A.H.A. T. Asbroek, L. Conteh, B.R. Kirkwood, S.R. Meek, Mobile health (mHealth) approaches and lessons for increased performance and retention of community health workers in low- and middle-income countries: a review, *J. Med. Internet Res.* 15 (2013) e17, <https://doi.org/10.2196/JMIR.2130>.
- [5] E. Osei, T.P. Mashamba-Thompson, Mobile health applications for disease screening and treatment support in low-and middle-income countries: a narrative review, *Heliyon* 7 (2021) e06639, <https://doi.org/10.1016/j.heliyon.2021.e06639>.
- [6] K. Hurt, R.J. Walker, J.A. Campbell, L.E. Egede, mHealth interventions in low and middle-income countries: a systematic review, *Glob. J. Health Sci.* 8 (2016) 183, <https://doi.org/10.5539/gjhs.v8n9p183>.
- [7] A. Roda, E. Michelini, M. Zangheri, M. Di Fusco, D. Calabria, P. Simoni, Smartphone-based biosensors: a critical review and perspectives, *TrAC Trends Anal. Chem.* 79 (2016) 317–325, <https://doi.org/10.1016/J.TRAC.2015.10.019>.
- [8] Z. Geng, X. Zhang, Z. Fan, X. Lv, Y. Su, H. Chen, Recent progress in optical biosensors based on smartphone platforms, *Sensors* 17 (2017), <https://doi.org/10.3390/S17112449>.
- [9] G. Xing, J. Ai, N. Wang, Q. Pu, Recent progress of smartphone-assisted microfluidic sensors for point of care testing, *TrAC Trends Anal. Chem.* 157 (2022) 116792, <https://doi.org/10.1016/J.TRAC.2022.116792>.
- [10] K. Kalinowska, W. Wojnowski, M. Tobiszewski, Smartphones as tools for equitable food quality assessment, *Trends Food Sci. Technol.* 111 (2021) 271–279, <https://doi.org/10.1016/J.TIFS.2021.02.068>.
- [11] E. Chao, C.K. Meenan, L.K. Ferris, Smartphone-based applications for skin monitoring and melanoma detection, *Dermatol. Clin.* 35 (2017) 551–557, <https://doi.org/10.1016/j.det.2017.06.014>.
- [12] R. Yu, G. Qiu, Y.B. Zhao, D. Freudemann, B. Fisher, X. Wang, J. Wang, A portable and smartphone-based plasmonic system for on-site measurement of airborne redox-active compounds by light-initiated redox reaction, *Sensors Actuators B Chem* 371 (2022) 132505, <https://doi.org/10.1016/J.SNB.2022.132505>.
- [13] T. Das, M. Mohar, Development of a smartphone-based real time cost-effective VOC sensor, *Heliyon* 6 (2020) e05167, <https://doi.org/10.1016/j.heliyon.2020.e05167>.
- [14] S. Srivastava, V. Sharma, Ultra-portable, smartphone-based spectrometer for heavy metal concentration measurement in drinking water samples, *Appl. Water Sci.* 11 (2021) 1–8, <https://doi.org/10.1007/s13201-021-01519-w>.
- [15] K. Xu, Q. Chen, Y. Zhao, C. Ge, S. Lin, J. Liao, Cost-effective, wireless, and portable smartphone-based electrochemical system for on-site monitoring and spatial mapping of the nitrite contamination in water, *Sensors Actuators B Chem* 319 (2020) 128221, <https://doi.org/10.1016/j.snb.2020.128221>.
- [16] A. Bayram, N. Horzum, A.U. Metin, V. Kilic, M.E. Solmaz, Colorimetric bisphenol-a detection with a portable smartphone-based spectrometer, *IEEE Sens. J.* 18 (2018) 5948–5955, <https://doi.org/10.1109/JSEN.2018.2843794>.
- [17] P.K. Smith, R.I. Krohn, G.T. Hermanson, A.K. Mallia, F.H. Gartner, M. D. Provenzano, E.K. Fujimoto, N.M. Goeke, B.J. Olson, D.C. Klenk, Measurement of protein using bicinchoninic acid, *Anal. Biochem.* 150 (1985) 76–85, [https://doi.org/10.1016/0003-2697\(85\)90442-7](https://doi.org/10.1016/0003-2697(85)90442-7).
- [18] K.J. Wiechelman, R.D. Braun, J.D. Fitzpatrick, Investigation of the bicinchoninic acid protein assay: identification of the groups responsible for color formation, *Anal. Biochem.* 175 (1988) 231–237, [https://doi.org/10.1016/0003-2697\(88\)90383-1](https://doi.org/10.1016/0003-2697(88)90383-1).
- [19] C.L. Kielkopf, W. Bauer, I.L. Urbatsch, Bradford assay for determining protein concentration, *Cold Spring Harb. Protoc.* 2020 (2020) 136–138, <https://doi.org/10.1101/PDB.PROT102269>.
- [20] S. Giguère, A.C. Polkes, Immunologic disorders in neonatal foals, *Vet. Clin. North Am. Equine Pract.* 21 (2005) 241–272, <https://doi.org/10.1016/j.cveq.2005.04.004>.
- [21] M. Abraham, J. Bauquier, Causes of equine perinatal mortality, *Vet. J.* 273 (2021) 105675, <https://doi.org/10.1016/j.tvjl.2021.105675>.
- [22] M. Mesas Gómez, B. Molina-Moya, B.C. de Araújo, A. Pallarès-Rusiñol, J. Ferrer-Dalmau, M.V. Boldrin Zanoni, J. Domínguez, E. Julian, M.I. Pividori, Mycobacterium detection method combining filtration, immunomagnetic separation, and electrochemical readout in a portable biosensing device, *Sensors Actuators B Chem.* 403 (2024) 135211, <https://doi.org/10.1016/j.snb.2023.135211>.
- [23] M. Mesas Gómez, B. Molina-Moya, B. de Araujo Souza, M.V. Boldrin Zanoni, E. Julián, J. Domínguez, M.I. Pividori, Improved biosensing of Legionella by integrating filtration and immunomagnetic separation of the bacteria retained in filters, *Microchim. Acta* 191 (2024) 82, <https://doi.org/10.1007/s00604-023-06122-1>.
- [24] S. Banik, S.K. MelanthotaArbaaz, J.M. Vaz, V.M. Kadambalithaya, I. Hussain, S. Dutta, N. Mazumder, Recent trends in smartphone-based detection for biomedical applications: a review, *Anal. Bioanal. Chem.* 413 (2021) 2389–2406, <https://doi.org/10.1007/s00216-021-03184-z>.